Lidar Turbulence Measurements for Wind Turbine Selection Studies : Design Turbulence

W. Barker[(1)], M. Harris[(2)],
M. Pitter[(3)], E. Burin des Roziers[(4)], J. Medley[(5)], C. Slinger[(6)],
[(1) – (6)]ZephIR lidar

(1) : Will Barker : ZephIR Ltd., The Old Barns, Fairoaks Farm, Hollybush, Ledbury, England, HR8 1EU.
willb@zephirlidar.com, Phone : +44 (0) 1531 651 000, Fax : +44 (0) 1644 430009.
(2) : Mike Harris : ZephIR Ltd., The Old Barns, Fairoaks Farm, Hollybush, Ledbury, England, HR8 1EU.
michaelh@ zephirlidar.com, Phone : +44 (0) 1531 651 000, Fax : +44 (0) 1644 430009.

Abstract

Comparison of turbulence measurements made by a ZephIR 300 VAD scanning wind lidar and a 91m IEC compliant anemometer mast are used to inform the analysis of the suitability of lidar measurements of turbulence for use in calculating effective turbulence in wind turbine selection studies following IEC 61400-1 and the Frandsen method. The deviation in turbulence measurements observed between the lidar and mast recorded over a full calendar year in the wind speed ranges applicable is used to determine bounds on deviation in the turbulence classification results for a typical eight turbine wind farm layout in non-complex terrain. Deviation in the design equivalent turbulence levels assessed at each turbine location for the range of deviation observed in mean turbulence measured by the lidar is shown to be small with respect to the turbulence bands used in the turbine classification. The turbulence spectrum measured by the lidar in neutral conditions is shown to match that of relevance in the turbine selection methodology particularly where the spatial filtering of the turbine rotor is taken into consideration.

1 Introduction

The use of lidar wind speed measurements in wind energy project methodologies has been demonstrated to provide advantages over traditional mast anemometry in terms of cost, logistics and accuracy. In this paper the suitability of lidar turbulence measurements is established in the context of an industry standard turbine selection methodology and also in terms of the turbulence spectra that are of relevance in the application. In selecting a turbine for a wind farm, turbulence measurements and modelled wake added turbulence are combined to assess the design turbulence levels at the turbine locations against manufacturer specifications. The turbulence measurements used are restricted to the neutral climatic conditions that predominantly occur during higher wind speed periods. This has implications in terms of the length-scales of turbulence that are relevant in turbulence measurements used to inform the selection of wind turbines. In this study the suitability of lidar turbulence measurements for this application is investigated at the ten minute mean level and also at the spectral level. Lidar is increasingly being used as the sole source of site measured wind data. Where this measurement strategy is applied it is important that the wind parameters measured by the lidar are of a suitable nature and quality to fulfill all of the analysis requirements of the wind project. Establishing the suitability of lidar turbulence measurements for use in turbine selection studies lends support to the use of lidar as a sole data source in wind energy projects demonstrating that the benefits afforded by lidar can be attained without compromising accuracy.

2 Design Turbulence Calculations

Design turbulence assessments for prospective wind turbine locations are generally carried out at the pre-construction analysis stage following various editions of IEC 61400-1 [1] – [3], or the Deutsches Institut für Bautechnik standard (DIBt) [4]. The analysis may be carried out using in-house tools that follow these standards or using a number of industry standard tools, for example WindFarmer [5], that implement the design turbulence calculations within a suite of design tools. Wind turbine models are classified by the manufacturer following IEC 61400-1 according to bandings of reference mean wind speed and turbulence intensity within which the turbine is designed to operate. The basic parameters for wind turbine classes are shown reproduced from [3] in Table 1. In assessing the suitability of a particular combination of location and wind turbine the aim is to determine whether the wind speed and turbulence at the location are within the classification banding for the turbine under consideration. The turbulence intensity at 15 m/s is used in the design turbulence calculations to define the characteristic standard deviation (σ_1) bands against which the turbine is classified in terms of wind turbulence. Following [3] :

$$\sigma_1 = I_{15}(5.6 + 0.75v) \qquad \text{Equation 1}$$

Where : I_{15} is the turbulence intensity at 15 m/s

v is the wind speed [m/s]

Wind turbine class		I	II	III	S
V_{ref}	(m/s)	50	42,5	37,5	Values
A	I_{ref} (-)	0,16			specified
B	I_{ref} (-)	0,14			by the
C	I_{ref} (-)	0,12			designer

Table 1 : Basic Parameters for Wind Turbine Classes Reproduced from [3]

In Table 1, the parameter values apply at hub height and :

V_{ref} is the reference wind speed average over 10 minutes

A designates the category for higher turbulence characteristics

B designates the category for medium turbulence characteristics

C designates the category for lower turbulence characteristics

I_{ref} is the expected value of the turbulence intensity at 15 m/s

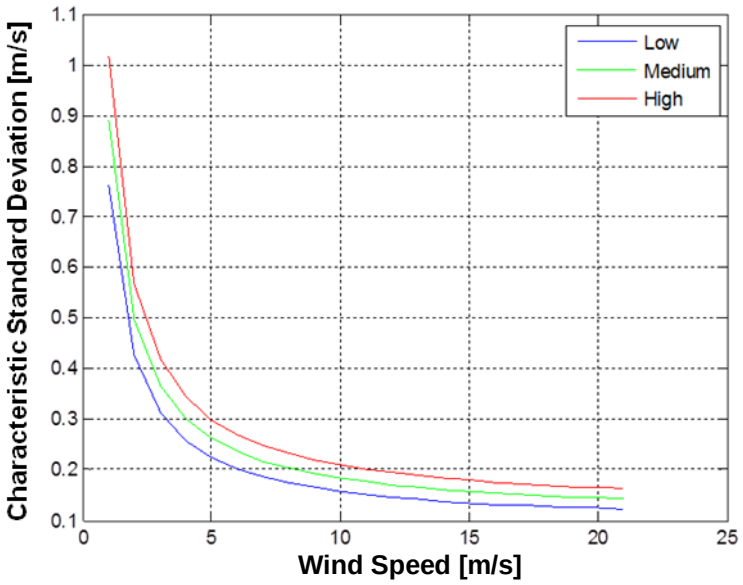

Figure 1 : Characteristic Standard Deviation Bands for Turbine Classification

The characteristic standard deviation bands are shown in Figure 1 following [3] where the bands are determined using the reference turbulence intensity values in Table 1 :

Low : $I_{15} = 0.12$, Medium : $I_{15} = 0.14$, High : $I_{15} = 0.16$

The site measured turbulence is used in the design turbulence calculations in the form of measured values of standard deviation and standard deviation of wind speed standard deviation (σσ) binned by direction and wind speed. These values are used to calculate the *Effective Turbulence* in each bin, Equation 2 :

$$\sigma eff_{i,j} = \sqrt{\frac{v_{hub,i}^2}{\left(1.5 + 0.8\frac{d_j}{\sqrt{c_t\left(v_{hub,i}\right)}}\right)^2} + \sigma rep_{i,j}^2} \qquad \text{Equation 2}$$

Where :

d_j is the distance to the neighboring turbine that causes the wake in direction bin j normalized by the rotor diameter of the turbine causing the wake.

$\sigma rep_{i.j}$ is the representative ambient wind speed standard deviation in wind direction bin j and wind speed bin i.

$$\sigma rep_{i,j} = \overline{\sigma_{i,j}} + 1.28\sigma\sigma_{i,j} \qquad \text{Equation 3}$$

Where :

$\overline{\sigma_{i,j}}$ is the mean measured wind speed standard deviation in wind speed bin I and wind direction bin j.

$\sigma\sigma_{i,j}$ is the standard deviation of the wind speed standard deviation in wind speed bin i and wind direction bin j.

The effective turbulence consists of the quadrature summation of a wake added term and the representative ambient wind speed standard deviation. The wake added term is independent of the measured turbulence and is calculated using the wind speed, turbine specific thrust curve and the separation of the turbines in the direction of the mean flow. An example of the constituent components of the effective turbulence is shown in Figure 2.

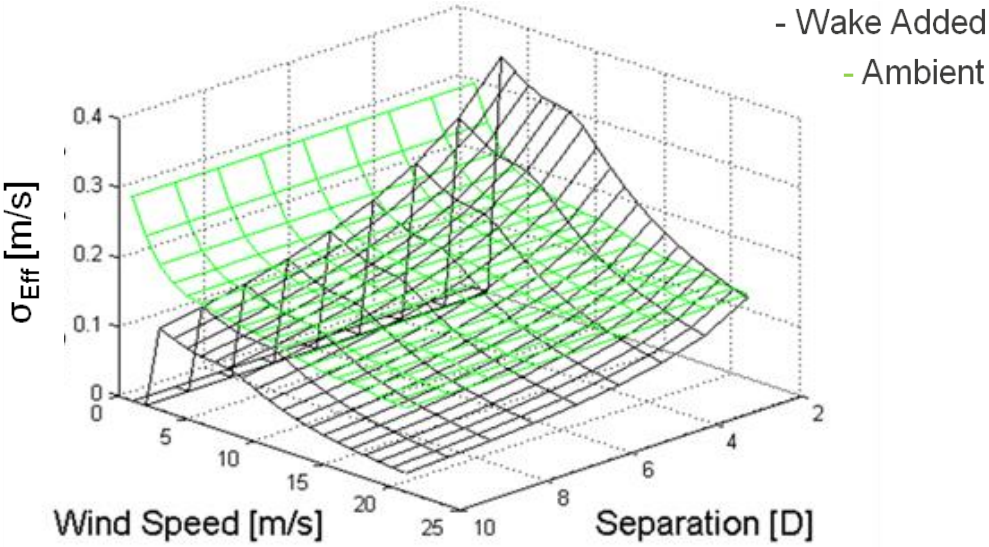

Figure 2 : Example Effective Turbulence Ambient and Wake Added Components

In selecting a wind turbine for a site the calculated effective turbulence should be below the characteristic turbulence associated with the design classification of the turbine for hub-height wind speeds between $0.2V_{ref}$ and $0.4V_{ref}$. V_{ref} is the reference wind speed associated with the design classification of the turbine. The following reference wind speed bands can be calculated by class from Table 1 :

Class I : 10.0 – 20.0 m/s, Class II : 8.5 – 17.0 m/s, Class III : 7.5 – 15.0 m/s

Figure 3 shows an example calculation for a class IIIB turbine validated against the results from WindFarmer [5]. The plot suggests that the turbine in this example is unsuitable for the proposed location.

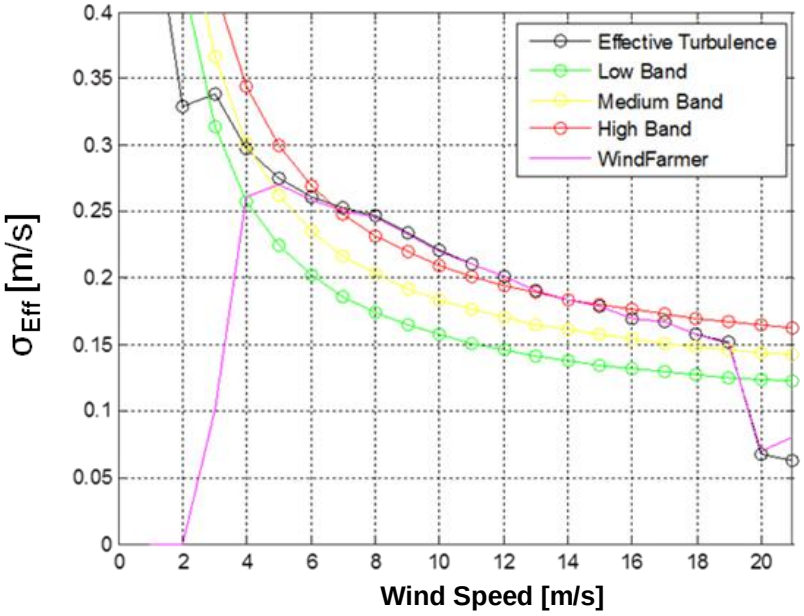

Figure 3 : Example Design Turbulence Assessment

3 Aims and Methodology

In order to assess the suitability of ZephIR 300 lidar data for use in design turbulence calculations, co-located data measured by ZephIR 300 and a 91m IEC compliant anemometer mast spanning a full calendar year, as detailed in [6] and [7], is analysed with a view to determining the following :

- The deviation in measured standard deviation (σ) observed for the ZephIR in the wind speed ranges associated with the wind turbine classes.
- The deviation in measured standard deviation of standard deviation (σσ) observed for the ZephIR in the wind speed ranges associated with the wind turbine classes.
- Bounds on the effects of these deviations in the end result of applying the design turbulence calculations for the type of site under consideration.
- Whether the bounds determined suggest that the ZephIR data can be used with confidence in the design turbulence calculations in place of cup anemometer data for the type of site under consideration.

The calculations in IEC 61400-1 [3] for the prediction of effective turbulence for a wind turbine location follow those presented by Frandsen [8] and are based on an assumption of neutral atmospheric stability. Neutral atmospheric conditions are predominant at higher wind speeds. This is the rationale behind the definition of characteristic turbulence in IEC 61400-1 [3] using a value associated high wind speed, 15 m/s, and the application of the wind speed ranges associated with the turbine classes in Table 1 which exclude low wind speeds. Three turbulence spectra definitions for application in design load calculations for the classification of wind turbines are also included across the IEC 61400-1 editions. These are the *Isotropic Von Karman* [9], *Mann Uniform Shear* [10] and *Kaimal* [11] spectral models. Mann's model is formulated using the Isotropic Von Karman model and both are formulated for neutral conditions. Although the Kaimal spectrum is applicable across atmospheric stability conditions the parameters for the spectrum defined in IEC 61400-1 are those associated with neutral conditions. A coherence model is also included to account for the lateral spatial correlation structure of the longitudinal velocity component. Frandsen [12] presents criteria for testing the quality of turbulence models with respect to design load calculations and also applies the coherence model in IEC 61400-1 [3] to develop a model of the effect of the turbine rotor in filtering the turbulence spectrum. Based upon a model of turbulence spectra measured by a VAD scanning lidar presented by Wagner [13] the ability of ZephIR 300 to measure the turbulence spectrum relevant for design turbulence calculations is analysed in this paper by comparing the modelled lidar spectrum with the rotor filtered modelled turbulence spectrum.

4 Results

4.1 Measured Wind Speed Standard Deviation

The wind speed ranges associated with the turbine classifications in Table 1 together span the range 7.5 – 20.0 m/s. Figure 4 shows a regression of the mast and lidar measured standard deviation at 70.5m above ground level (AGL) measured at the Pershore test site. Figure 5 suggest that the relationship between the standard deviation measurements is relatively invariant with wind speed. The mean deviation measures for the data sets are shown in Table 2. Mean values in each wind speed bin are used in the design turbulence calculations. Table 2 suggests that a deviation of mean standard deviation of ≈ -4.0% may be representative of the relative performance of the ZephIR and mast within the wind speed range and associated with this application.

4.2 Standard Deviation of the Measured Wind Speed Standard Deviation

Figures 6 a) and b) show the distribution of the wind speed standard deviation measurements from the lidar and the cup anemometer from within the wind speed range of 7.5 – 20.0 m/s split into unstable and stable conditions respectively.

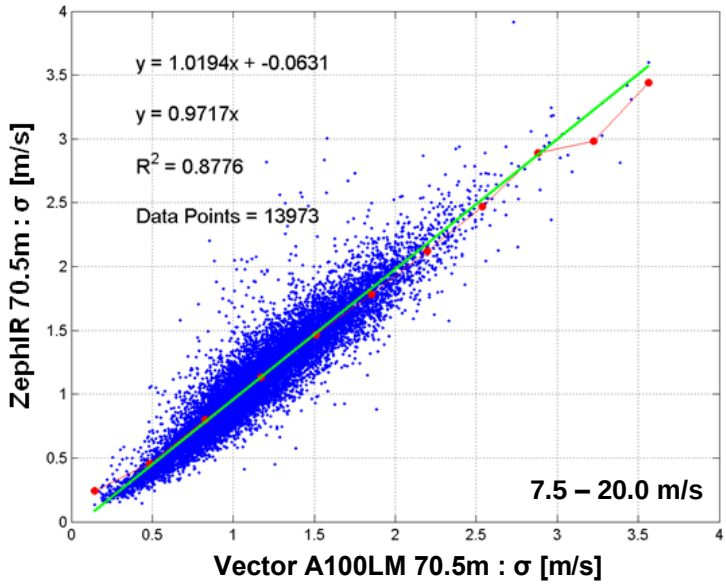

Figure 4 : Lidar Measured Turbulence vs Cup Measured Turbulence : 70.5m AGL

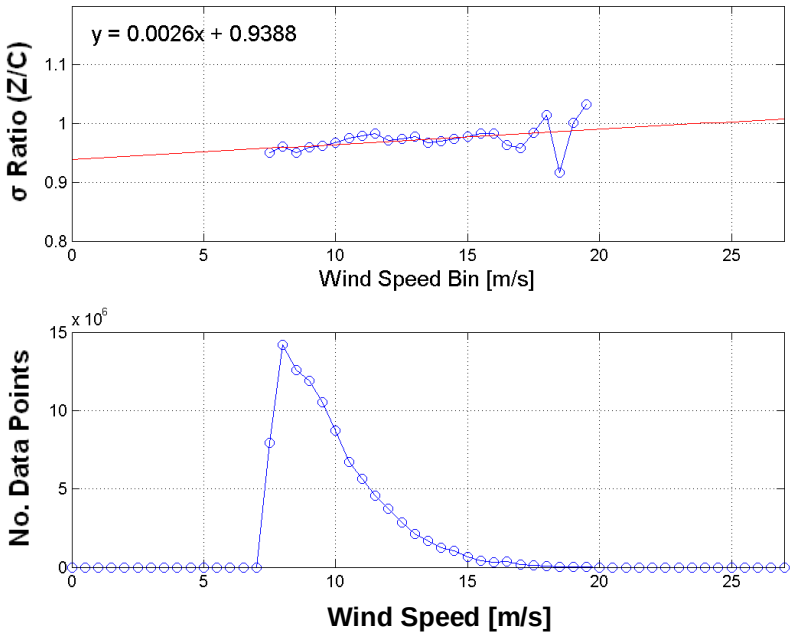

Figure 5 : Variation of Ratio of lidar and Cup Standard Deviation with Wind Speed

Wind Speed Range	Mean σ Deviation	Deviation of Mean σ	Mean of Mean WS Binned σ Ratio - 1.0	Average
[m/s]	(Z-C)/C [%]	(Z-C)/C [%]	[%]	[%]
7.5 - 20.0	-4.3	-3.4	-3.0	-3.6

Table 2 : Mean Deviation Measures for Wind Speed Standard Deviation Measured by the lidar and Cup Anemometer. Z = ZephIR 300, C = Cup Anemometer

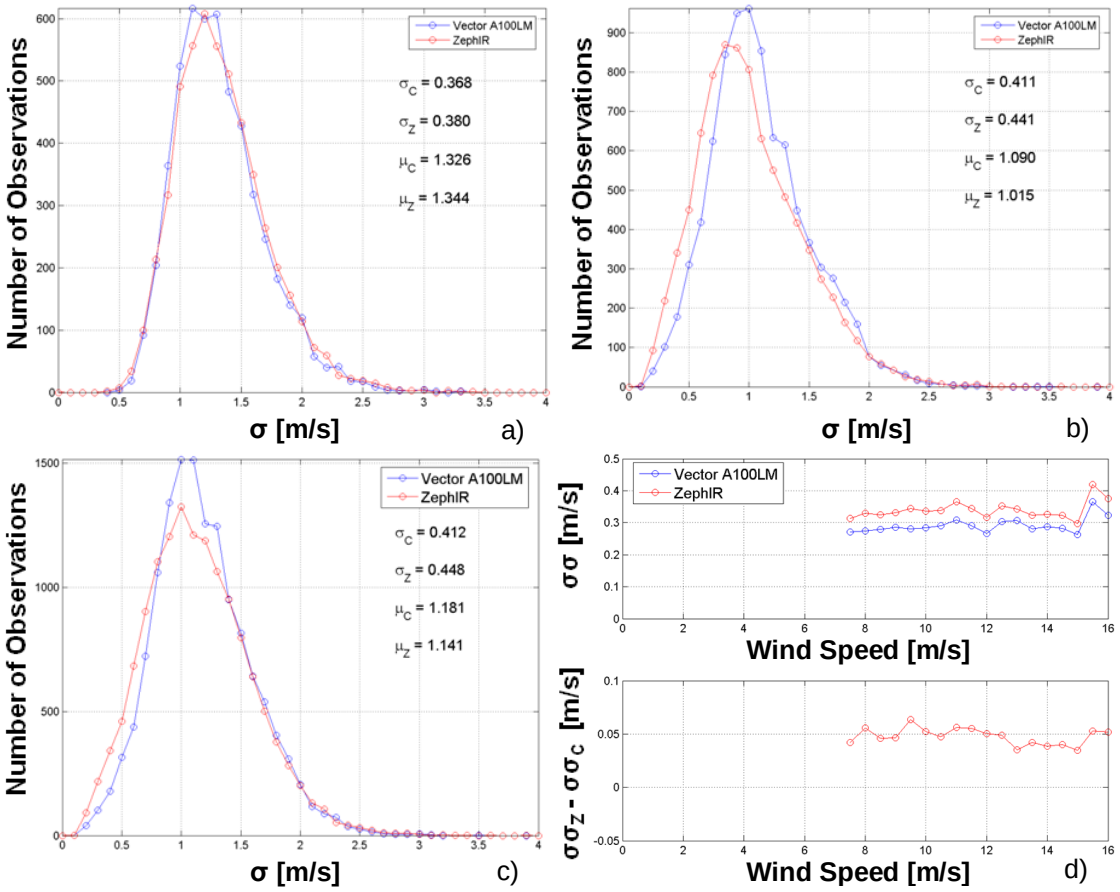

Figure 6 : Standard Deviation of Wind Speed Standard Deviation
a) 7.5 – 20.0 m/s : Unstable, b) 7.5 – 20.0 m/s : Stable, c) 7.5 – 20.0 m/s
d) Variation with Wind Speed, Z = ZephIR 300, C = Cup Anemometer

In unstable conditions the distributions from the two instruments can be seen to be very similar in terms of both the mean and standard deviation of the measurements. In stable conditions the distributions diverge with the lidar over-estimating the mean standard deviation compared to the cup anemometer and under-estimating the standard deviation of the measurements. This result is determined by the effect of variation in turbulent length-scale with stability on the lidar measurements as described in [13]. Figure 6 c) shows the overall distributions observed for the wind speed range associated with the design turbulence calculations. In this case the mean standard deviation values are closely matched but the standard deviation is over-estimated by the lidar. This is due to variation in stability around neutral conditions that may still occur to some degree at higher wind speeds. The deviation in the standard deviation of wind speed standard deviation (σσ) measured by the lidar and cup anemometer are shown in Table 3.

σσ Deviation 7.5 - 20.0 m/s		
(Z-C)/C [%]		
All	**Stable**	**Unstable**
8.74	7.30	3.26

Table 3 : Deviation in Standard Deviation of Wind Speed Standard Deviation Measured by the lidar and Cup Anemometer. Z = ZephIR 300, C = Cup Anemometer

Over-estimation of σσ by the lidar is increased in the overall distribution due to superposition of distributions for stable and unstable conditions which widens the overall distribution. Figure 6 d)

shows that over-estimate is invariant with wind speed. Placing bounds on a maximum value for this over-estimate from the plots in the wind speed range of interest gives a value of around +0.05 m/s.

4.3 Effect of Measurement Deviation on the Design Turbulence Calculations

Figure 8 compares the effective turbulence calculations for a hypothetical wind farm layout at the Pershore test site based on the measured data from the site. The turbine considered is class IIB with a rotor diameter of 80.0m. Figure 8 d) shows the results of the calculation using the cup anemometer measurements from the test site. Figure 8 e) shows the results of the calculation using the lidar measurements from the test site. Only data points where concurrent data is available from both the cup anemometer and lidar is used in these calculations. Figure 8 f) shows the deviation in the calculated effective turbulence where the cup anemometer data has been perturbed by the mean scaling of standard deviation and mean bias in standard deviation of standard deviation determined for the lidar in Sections 4.1 and 4.2. The results are expressed as a percentage of the minimum difference between classification bands in each wind speed bin. Figure 8 g) shows the same plot for the deviation between cup anemometer and measured lidar data. It can be seen from these plots that in the wind speed range of relevance for the design turbulence calculations the effective turbulence predicted from the lidar deviates by no more than 10% of the minimum difference between the turbulence bands used to classify the wind turbine. The difference between Figures 8 f) and g) with wind speed are likely to be due to the statistical effect of small bin populations after binning the measured standard deviation by wind speed and direction.

4.4 Turbulence Spectra for Design Turbulence Calculations

Figure 7 a) shows the filtering effect of the lidar scan at 70m AGL on the IEC Kaimal (1972) turbulence spectrum following [13]. Figure 7 b) Shows the filtering effect of the rotor on the IEC Kaimal (1972) turbulence spectrum for an 80.0m diameter rotor following [8]. The rotor filters out high frequency components from the stream-wise turbulence spectrum through the lateral coherence of the turbulence. This is due to the effect of small scale turbulence in the stream-wise direction canceling when integrated across the rotor area. It can be seen from the figures that the lidar is capable of measuring a turbulence spectrum that encompasses the rotor filtered spectrum. As the variance of the wind speed measurement appears as the integral of the un-normalised form of the spectrum in Figure 8 the turbulence of relevance in this application will be measured accurately by the lidar.

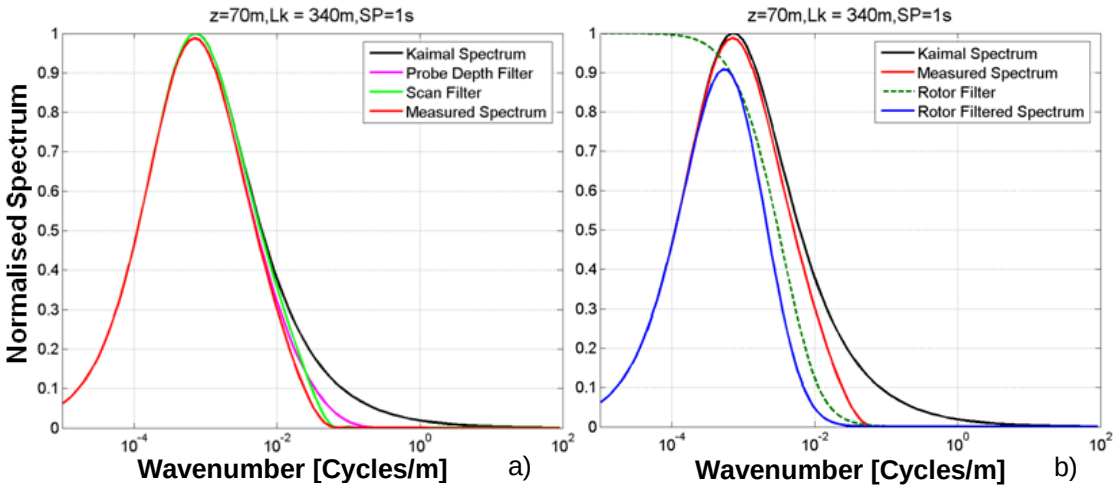

Figure 7 : IEC Kaimal (1972) Spectrum with a) lidar and b) Turbine Rotor Filter Models

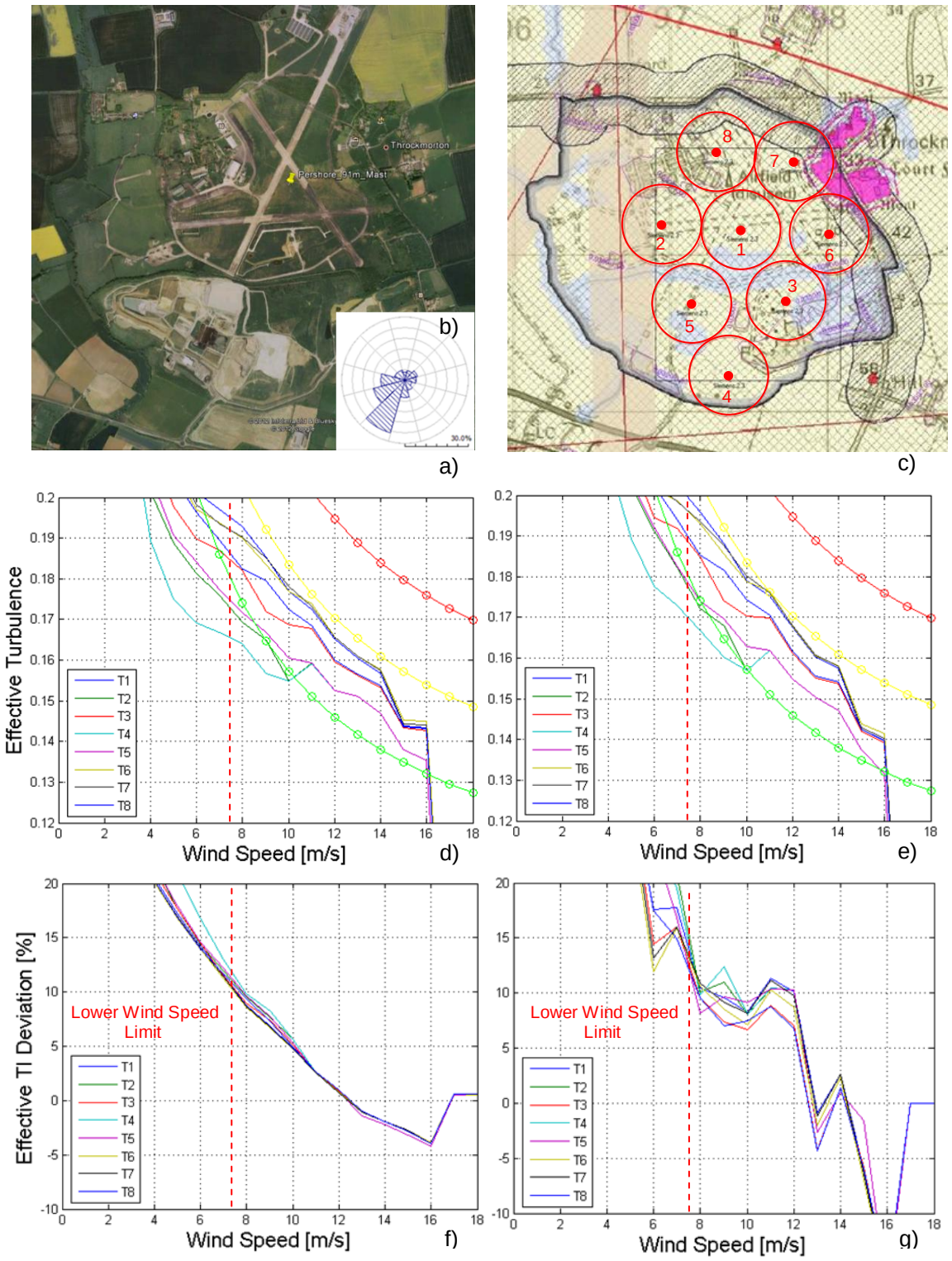

Figure 8 : a) Pershore Test Site, b) Wind Direction Distribution, c) Eight Turbine Layout, d) Effective Turbulence Calculated from Cup Anemometer Data, e) Effective Turbulence Calculated from lidar data, f) & g) Deviation in Calculated Effective TI as Percentage of Minimum Difference Between Classification Bands : f) Cup vs Cup Perturbed by mean lidar/cup σ ratio and σσ bias, g) Cup vs lidar Measured.

5 Conclusions

The ZephIR 300 lidar has been demonstrated to perform well compared to a class 1 cup anemometer in measuring the turbulence statistics required for the estimation of effective turbulence following the industry standard methodology in IEC 61400-1 [3] and [8]. A deviation in measured mean wind speed standard deviation of -4% relative to the cup anemometer and a bias in standard deviation of wind speed standard deviation of 0.05 m/s are observed in the wind speed ranges required by the methodology. When applied to a real-world wind farm layout in non-complex terrain the effective turbulence predicted using a year of concurrent data from the lidar and cup anemometer deviate by no more than 10% of the minimum difference between the turbine classification bands across the wind speed range. The lidar and cup anemometer turbulence measurements are therefore effectively equivalent in this application as using the lidar measurements to assess effective turbulence will not move the turbine selection into another classification band unless the results are already at the boundary of the class. The modeled turbulence spectrum measured by the lidar is shown not to deviate significantly from the standard spectra for turbine design load calculations included in IEC 61400-1. When the filtering of the turbine rotor is taken into account the lidar is shown to be capable of measuring the total turbulence spectrum sensed by the wind turbine rotor.

References

[1] IEC 61400-1 (1998) International Standard *: Wind turbines, Part 1: Design Requirements.* Edition 2.0 1998, International Electrotechnical Commission.

[2] IEC 61400-1 (2005), International Standard *: Wind turbines, Part 1: Design Requirements.* Edition 3.0 2005, International Electrotechnical Commission.

[3] IEC 61400-1 (2005), International Standard *: Wind turbines, Part 1: Design Requirements.* Edition 3.0 Amendment 2010, International Electrotechnical Commission.

[4] DIBt (Deutsches Institut für Bautechnik), *Richtlinie für Windenergieanlagen, Einwirkungen und Standsicherheitsnachweise für Turm und Gründung*, Schriften des Deutschen Instituts für Bautechnik", Reihe B, Heft 8; 2004.

[5] *GH WindFarmer : Wind Farm Design Software : Theory Manual V4.2.* Garrad Hassan and Partners Ltd. 2011.

[6] W.Barker et.al. "*Can Lidars Measure Turbulence? Comparison Between ZephIR 300 and an IEC Compliant Anemometer Mast*", Natural Power/ZephIR Ltd., EWEA 2012.

[7] W. Barker, M. Harris et. al., *Lidar Turbulence Measurements for Wind Farm Energy Yield Analysis*, Natural Power/ ZephIR Ltd., EWEA 2013.

[8] Sten Tronæs Frandsen, *Turbulence and Turbulence-generated Structural Loading in Wind Turbine Clusters*, Risø-R-1188(EN), 2005

[9] T. von Karman, *Progress in the statistical theory of turbulence*, Proc. Nat. Acad. Sci., v. 34, 1948, pp. 530-539.

[10] J. Mann, *The spatial structure of neutral atmospheric surface-layer turbulence*, J. of Fluid Mech., v. 273, 1994, pp. 141-168.

[11] J.C. Kaimal, J.C. Wyngaard, Y. Izumi, and O.R. Cote, *Spectral characteristics of surface-layer turbulence*, Q.J.R. Meteorol. Soc., v. 98, 1972, pp. 563-598.

[12] S. Frandsen, H. E. Jorgensen and J. D. Sorensen, *Relevant Criteria for Testing the Quality of Turbulence Models*, Journal of solar energy engineering, Vol. 130, Nº 3, pp. 1016, 2008.

[13] R. Wagner, T. Mikkelsen, M. Courtney, *Investigation of Turbulence Measurements with a Continuous Wave, Conically Scanning LiDAR*, Wind Enegy Division, Risø DTU. Risø-R-1682(EN), 2009.